

# A unified description of collective magnetic excitations

Benjamin W. Zingsem,<sup>1,2</sup> Michael Winklhofer,<sup>1,3</sup> Ralf Meckenstock,<sup>1</sup> and Michael Farle<sup>1,4</sup>

<sup>1</sup>*Faculty of Physics and Center for Nanointegration (CENIDE),*

*University Duisburg-Essen, 47057 Duisburg, Germany*

<sup>2</sup>*Ernst Ruska-Centre for Microscopy and Spectroscopy*

*with Electrons and Peter Grünberg Institute,*

*Forschungszentrum Jülich GmbH, 52425 Jülich, Germany*

<sup>3</sup>*IBU/School of Mathematics and Science, University of Oldenburg,*

*Carl-von-Ossietzky-Strasse 9-11, D-26129 Oldenburg, Germany*

<sup>4</sup>*Center for Functionalized Magnetic Materials,*

*Immanuel Kant Baltic Federal University,*

*236041 Kaliningrad, Russian Federation*

## Abstract

In this work, we define a set of analytic tools to describe the dynamic response of the magnetization to small perturbations, which can be used on its own or in combination with micromagnetic simulations and does not require saturation. We present a general analytic description of the ferromagnetic high frequency susceptibility tensor to describe angular as well as frequency dependent ferromagnetic resonance spectra and account for asymmetries in the line shape. Furthermore, we expand this model to reciprocal space and show how it describes the magnon dispersion. Finally we suggest a trajectory dependent solving tool to describe the equilibrium states of the magnetization.

## I. INTRODUCTION

Many solutions of the Ferromagnetic high frequency susceptibility (Polder-) tensor<sup>1</sup> have been formulated. Mostly these solutions represent simplified versions to suit particular problems, such as a certain energy landscape, a certain kind of coupling or a specific symmetry. In this work we formulate a generalized linearization of the Landau-Lifshitz-Gilbert<sup>2,3</sup> equations (LLG), which does not require symmetry assumptions and is applicable regardless of the coupling as well as the types of damping present in the system. It allows one to start with a general formulation of the free energy density of ferromagnets, including all magnetic interactions which might be present in the magnetic material, e.g. exchange, dipole-dipole, Dzyaloshinskii-Moriya interaction, anisotropies, etc. and can be expanded to antiferromagnets and multilayer artificial antiferromagnets in the usual way<sup>4-6</sup>. The conventional approaches mostly involve solving large systems of equations, linearizing at different points in the calculation in order to formulate the high frequency susceptibility<sup>1,7,8</sup>. This is avoided here, by applying a straight forward linearization through series expansion of the LLG. Furthermore this algorithm is formulated to cover the entire magnon dispersion, including ferromagnetic resonance modes as well as traveling waves with non-zero wave-vectors.

In the second part we present a model that can be used to calculate the equilibrium orientations of the magnetization, using an algorithm that closely resembles the actual measurement procedures used in ferromagnetic resonance measurements. Following a gradient of the energy landscape imposed on the magnetization, this model can be used to describe meta-stable and stable equilibrium states of the magnetization even for fields that are not applied along symmetry directions.

Neglecting thermal fluctuations, a combination of those models can be used to make accurate predictions about the magnetodynamic properties of ferromagnetic systems.

## II. ANALYTIC MODEL

### A. The ferromagnetic high frequency susceptibility tensor

In the derivation presented here we assume a system that is described by one macro-spin<sup>1,6-10</sup>  $\vec{M}$  which is subjected to one effective magnetic field  $\vec{B}$  yielding one high frequency

susceptibility tensor  $\underline{\chi}_{\text{hf}}$ . This model therefore as derived here is designed to describe a fully saturated sample. It is not limited to a single magnetization though and can be applied to a set of macro-spins where the local effective magnetic field is known at each site. In that case the total high frequency susceptibility would be given as  $\chi = \sum_n \chi_n$  where  $\chi_n$  is the high frequency susceptibility of the  $n^{\text{th}}$  macro-spin  $\vec{M}_n$  due to the field  $\vec{B}_n$  it is exposed to. This can be used for non saturated systems and samples with inhomogeneous magnetization or magnetic nanoparticle configurations.

In order to derive the full tensor we start from the Landau-Lifshitz-Gilbert Equation 1 using the Polder-Ansatz<sup>1</sup> as shown in eq. 2

$$\vec{L} := -\gamma \vec{M} \times \vec{B} - \frac{\alpha}{M} \vec{M} \times \dot{\vec{M}} - \dot{\vec{M}} = 0 \quad (1)$$

$$\begin{aligned} \vec{M}(t) &:= \vec{M}(M, \theta_M, \varphi_M) + \vec{m} \exp(i\omega t) \\ \vec{B}(t) &:= \vec{B}(B, \theta_B, \varphi_B) + \vec{b} \exp(i\omega t) \end{aligned} \quad (2)$$

Considering the dynamic excitation and response quantities  $\vec{m}$  and  $\vec{b}$  to be sufficiently small, the ferromagnetic high-frequency susceptibility  $\underline{\chi}_{\text{hf}}$  can be expressed as a linear tensor

$$\vec{m} = \underline{\chi}_{\text{hf}} \cdot \vec{b} \quad (3)$$

where linear means, that  $\underline{\chi}_{\text{hf}}$  does not depend on  $\vec{m}$  and  $\vec{b}$ . This is usually the case for microwave fields  $\|\vec{b}\| < 1 \text{ mT}$ . To obtain the magnetic flux that the magnetization is exposed to, we consider the magnetic contribution to the free energy per unit volume  $F(\vec{B}_{\text{appl}}, \vec{M})$  where  $\vec{B}_{\text{appl}}$  corresponds to the applied magnetic field and  $\vec{M}$  is the magnetization vector as discussed in the literature (See for example<sup>10</sup>). The Helmholtz free energy density  $F$  usually contains an anisotropic contribution due to the crystal lattice, particularly spin orbit interaction, as well as several other contributions that arise from surfaces/interfaces, the shape of the sample and the Zeeman-Energy. In this generalized approach the nature of these magnetic energies almost does not matter. The only necessary requirement is that the first

and second derivatives used in eq. 4 exist. The total magnetic flux is then given as

$$\begin{aligned}\vec{B}(t) = & \nabla_{\vec{M}} F(\vec{B}_{\text{appl}}, \vec{M}) \\ & + \underline{J}_{\vec{M}} \left( \nabla_{\vec{M}} F(\vec{B}_{\text{appl}}, \vec{M}) \right) \cdot \vec{m} \exp(i\omega t) \\ & + \vec{b} \exp(i\omega t)\end{aligned}\quad (4)$$

where  $\nabla_{\vec{M}} F(\vec{B}_{\text{appl}}, \vec{M})$  is the anisotropy-field and  $\underline{J}_{\vec{M}} \left( \nabla_{\vec{M}} F(\vec{B}_{\text{appl}}, \vec{M}) \right)$  the response function that accounts for a field caused by a precessing  $\vec{m}$ , where  $\nabla_{\vec{M}}$  is the gradient in  $\vec{M}$  and  $\underline{J}_{\vec{M}}$  the Jacobian matrix in  $\vec{M}$ . Using this we can now go back to eq. 1 and obtain

$$\begin{aligned}\vec{L} \rightarrow \vec{L}(\vec{b}, \vec{m}) = & -\gamma \vec{M}(t) \times \vec{B}(t) \\ & - \frac{\alpha}{M} \vec{M}(t) \times \dot{\vec{M}}(t) - \dot{\vec{M}}(t) \stackrel{!}{=} 0 \forall t\end{aligned}\quad (5)$$

which defines the hyper-plane in which all dynamic motion of the magnetization takes place. Since  $\vec{m}$  and  $\vec{b}$  are small, as defined in 3 we can now approximate  $\vec{L}(\vec{b}, \vec{m})$  by using a Taylor-expansion around  $\vec{L}(\vec{b} = \vec{0}, \vec{m} = \vec{0})$  to obtain

$$\vec{L}(\vec{b}, \vec{m}) \approx \underbrace{\vec{L}(\vec{0}, \vec{0})}_{\vec{0}} + \underline{J}_{\vec{b}, \vec{m}} \cdot (b_x, b_y, b_z, m_x, m_y, m_z)^\top \quad (6)$$

This leads to the system of equations 7,

$$\vec{0} \stackrel{!}{=} \underline{J}_{\vec{b}, \vec{m}} \cdot (b_x, b_y, b_z, m_x, m_y, m_z)^\top \quad (7)$$

where  $\underline{J}_{\vec{b}, \vec{m}} = \underline{J}_{(b_x, b_y, b_z, m_x, m_y, m_z)^\top} \left( \vec{L}(\vec{b}, \vec{m}) \right)$  is the Jacobian matrix of  $\vec{L}$  in  $\vec{b}$  and  $\vec{m}$ . Eq. 7 can then be further decomposed into

$$\begin{aligned}\vec{0} = & \underline{J}_{\vec{b}} \cdot \vec{b} + \underline{J}_{\vec{m}} \cdot \vec{m} \\ \vec{m} = & - \left( \left( \underline{J}_{\vec{m}} \right)^{-1} \cdot \underline{J}_{\vec{b}} \right) \cdot \vec{b}\end{aligned}\quad (8)$$

where  $\underline{J}_{\vec{m}}$  and  $\underline{J}_{\vec{b}}$  are the Jacobian matrices in  $\vec{m}$  and  $\vec{b}$  respectively. By comparison to eq. 3 we find

$$\underline{\chi}_{\text{hf}} = - \left( \left( \underline{J}_{\vec{m}} \right)^{-1} \cdot \underline{J}_{\vec{b}} \right) \quad (9)$$

which we refer to as the complete analytic solution of the ferromagnetic high-frequency

susceptibility. Note that this approach is independent of the form of the free energy functional. Since we obtain the full tensor without assumptions regarding its entries, we have to project it on the unit vectors  $\vec{u}_b$  and  $\vec{u}_m$  that represent an excitation-measurement-pair of observables to obtain a representative spectrum. In a typical numerical evaluation one would assume  $\vec{u}_b$  to be parallel to the unit-vector in  $\phi$  direction of the applied field  $\vec{B}$  and  $\vec{u}_m$  to be parallel to the unit-vector in  $\phi$  direction of the magnetization vector in spherical coordinates. Nonparallel unit-vectors  $\vec{u}_b$  and  $\vec{u}_m$  can be used to account for nonuniform microwave fields. The angle between  $\vec{u}_b$  and  $\vec{u}_m$  represents an effective phase shift  $\Delta$  between the excitation and the response. This is illustrated in the inset in fig. 1. Such a phase shift can be created for instance by having the sample covered by a conductive layer in which the microwave creates an eddy current that in turn creates a phase shifted microwave signal that superimposes with the original one as described in<sup>11</sup>. The approach presented here was used in<sup>12</sup> to calculate asymmetric line shapes.

## B. Extension to reciprocal- $(\vec{k})$ -space and description of the magnon dispersion

The model presented above can be extended to reciprocal space in order to obtain the magnon dispersion. Accordingly, the spatial contributions to the energy landscape are included in the energy density formulation. Also the Ansatz has to be changed such that the dynamic magnetization has a spatial dependence. We imagine that the spatial distribution of the magnetization can be described as a constant part and a dynamic part where the dynamic part is a Fourier series. In contrast to the description by Suhl, where this Ansatz appears<sup>13</sup> we consider the amplitude for every  $\vec{k}$  to be small, such that we can perturb the system with a single  $\vec{k}$  at a time, yielding an Ansatz of the form

$$\vec{M}(t, x) := \vec{M}(M, \theta_M, \varphi_M) + m_{\vec{k}} \exp\left(i\omega t - \vec{k} \cdot \vec{x}\right) \quad (10)$$

where  $\vec{k}$  is the reciprocal vector for which the susceptibility is being calculated and  $\vec{x}$  is the spatial coordinate at which the wave is observed.

For example we can consider exchange energy contribution in a continuum model

$$F_{\text{ex}} = d^2 \frac{B_{\text{ex}}}{\|\vec{M}\|} \left( \vec{M}(t, x) \cdot \Delta \vec{M}(t, x) \right) \quad (11)$$

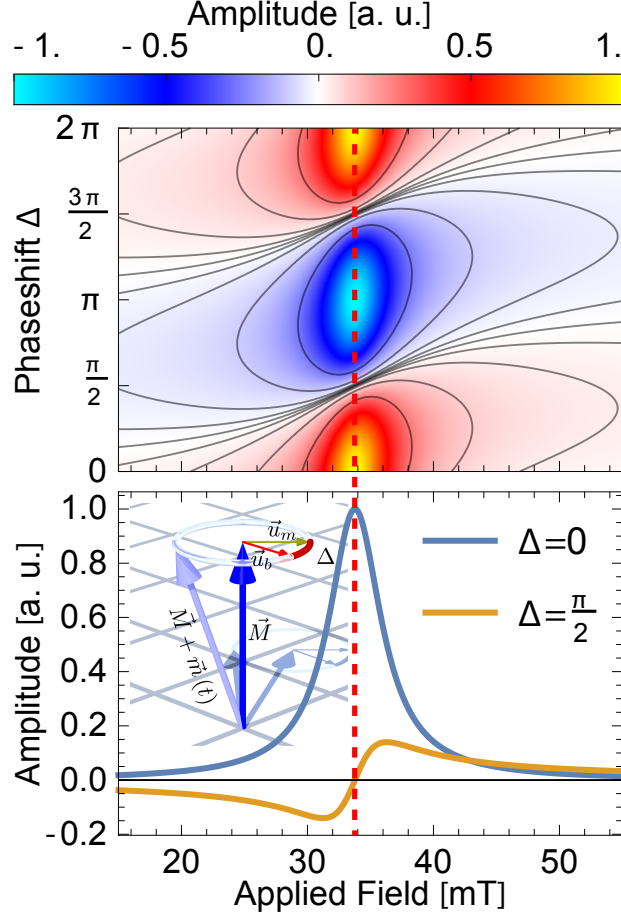


Figure 1: Top: Amplitude of the susceptibility as a function of the applied magnetic field and the phase-shift  $\Delta$ . At the angles  $\pi/2$  and  $3\pi/2$  the line-shape is fully anti-symmetric similar to the derivative of a Lorentz line-shape. In the vicinity of those angles the signal is asymmetric. At the angles 0 and  $2\pi$  the signal is symmetric with positive amplitude and at  $\pi$  the signal is symmetric with negative amplitude. Bottom: Selected lines at specific angles 0 and  $\frac{\pi}{2}$ . The inset illustrates the phase shift  $\Delta$  induced by choosing a nonparallel tuple of excitation measurement projection vectors  $\vec{u}_b$  and  $\vec{u}_m$  shown in the precession cone of the time dependent magnetization. For simplicity the precession is indicated as a circular motion normalized to the length of the unit vectors perpendicular to  $\vec{M}$ . In general it would be approximated to be elliptical and the opening of the cone is much smaller compared to the Magnetization vector.

and a  $\vec{k}$  dependent dipolar coupling to include dynamic aspects of dipolar interactions

$$F_{\text{Demag}} = \frac{1}{2}\mu_0 \left\| \vec{M} \right\| \frac{\vec{m}_k \cdot \vec{k}}{\left\| \vec{m} \right\|^2 \left\| \vec{k} \right\|^2} \vec{k} \cdot \vec{M}(t, x) \quad (12)$$

where  $d$  is the distance between two neighboring spins,  $B_{ex}$  is the exchange field they exert on each other and  $\Delta$  is the Laplace operator in real space. Adding this contribution to the

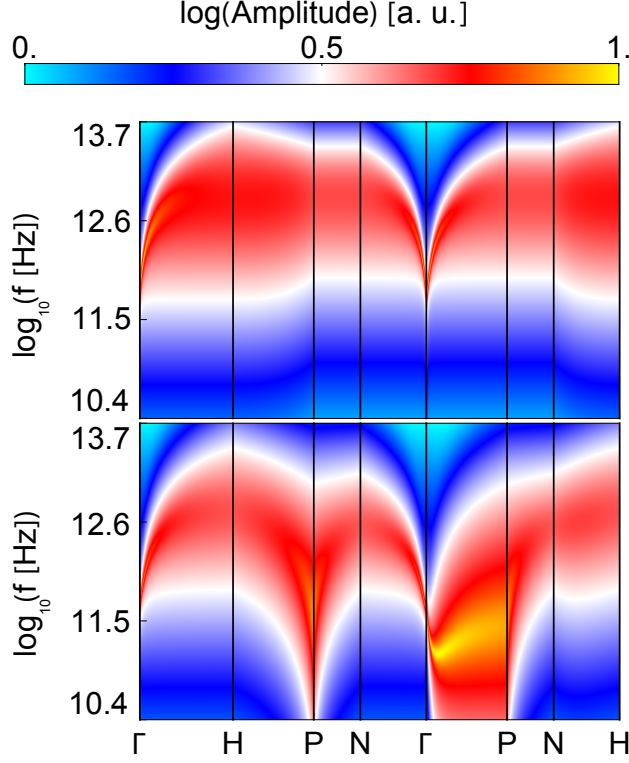


Figure 2: The magnon dispersion calculated for a bcc structure including a cubic anisotropy exchange and dipolar coupling (top) and for a similar system with an additional strong chiral<sup>14,15</sup> coupling (bottom).

Helmholtz energy density we can proceed as before and calculate the susceptibility for every  $\vec{k}$  in the Brillouin zone as shown exemplary in fig. 2. The results agree with the literature (see for instance<sup>16–20</sup>). For other spatial contributions such as anisotropic exchange and chiral coupling, the model can be applied in the same way.

### C. The equilibrium position of the magnetization

In order to use the result in eq. 9 to obtain the susceptibility it is necessary for  $\vec{M}(\theta_M, \phi_M)$  to locally minimize the free energy density. The orientation of the magnetization vector has to be determined from the shape of the free energy landscape including an applied magnetic field. In the following we present our recursive method to efficiently find these minima. In terms of infinitesimals this method can be viewed as a trajectory depended analytic solution. Due to its infinite recursion along a chosen trajectory however it resembles a second order newton algorithm, which is a numerical tool, and we therefore tend to call it a semi-analytic trajectory dependent solution of the equilibrium states of the magnetization.

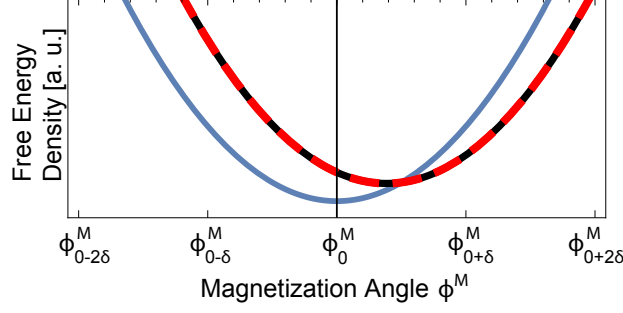


Figure 3: The environment of a minimum of the energy Landscape as a function of the Magnetization angle (blue) and the same energy landscape after changing the applied field angle  $\phi_B$  by a small quantity  $\delta$  (black) together with a Taylor expansion of the changed energy landscape around the the position  $\phi_0^M$  (red dashed). Note that the series expansion fits perfectly to the black curve around its minimum.

For certain paths in the applied field space, where the trajectory passes sufficiently far beyond a hard direction, the equilibrium angles are discontinuous if the Zeeman energy does not overcome the anisotropic contributions of this hard direction. This can lead to a hysteretic behavior of the magnetization depending on the trajectory of  $\vec{B}(\tau) := \vec{B}(B(\tau), \theta_B(\tau), \varphi_B(\tau))$ . To account for this behavior a solution representing the equilibrium angles must depend on the trajectory  $\vec{B}(\tau)$  and not only on a momentary configuration of  $\vec{B}$ . Without loss of generality we will only consider the equilibrium angles  $\{\theta_M, \varphi_M\}$  of the magnetization in spherical coordinates to minimize the free energy, since in many applications the norm of the magnetization may be considered constant. Once a minimizer  $\vec{\Omega}(\vec{B}(0)) = \{\theta_M, \varphi_M\}_0$  of the free energy  $F(\vec{B}, \vec{M})$  is known for a certain starting configuration  $\vec{B}(0)$ , a small change in  $\vec{B} \rightarrow \vec{B}(0 + \delta)$  that yields a small change in the position of the minimum of  $F(\vec{B}, \vec{M})$  can be accounted for by calculating a series expansion of  $F(\vec{B}(0 + \delta), \vec{M})$  at the position  $\{\theta_M, \varphi_M\}_0$  to the second order. The position of the minimum of this parabola will be close to the minimum  $\{\theta_M, \varphi_M\}_{0+\delta}$  of  $F(\vec{B}(0 + \delta), \vec{M})$ . In fact as  $\delta$  decreases the solution obtained this way will get closer to the exact minimum. This procedure is illustrated in fig. 3, where the free energy was defined to be  $F = \sin^2(2\phi_M) - 5\cos(\phi_B - \phi_M)$ . Since the function obtained from the series expansion is of quadratic order it can always be written in a form such that the vertex can

be directly extracted from the function. Therefore a recursive function of the form [13](#)

$$\begin{aligned}
\vec{\Omega} \left( \vec{B} (0 - \delta) \right) &= \vec{\Omega} \left( \vec{B} (0) \right) - \\
&\quad \underline{\underline{H}}_F^{-1} \Big|_{\vec{\Omega}(\vec{B}(0-\delta))} \cdot \vec{\nabla} F \Big|_{\vec{\Omega}(\vec{B}(0-\delta))} \\
\vec{\Omega} \left( \vec{B} (0 - 2\delta) \right) &= \vec{\Omega} \left( \vec{B} (0 - \delta) \right) - \\
&\quad \underline{\underline{H}}_F^{-1} \Big|_{\vec{\Omega}(\vec{B}(0-2\delta))} \cdot \vec{\nabla} F \Big|_{\vec{\Omega}(\vec{B}(0-2\delta))} \\
&\quad \dots
\end{aligned} \tag{13}$$

can be derived to describe the position of a minimum for certain trajectories  $\vec{B}(\tau)$ , where  $\underline{\underline{H}}_F$  is the Hessian Matrix of the free energy density that described the curvature and  $\vec{\nabla} F$  the gradient that describes the slope of the free energy. Conceptually this can be considered a second order Newton algorithm with the exception that it starts from a known position making the number of iterations required tend towards 1 as  $\delta$  gets small. To determine a minimizer that can be used as a starting point in eq. [13](#) the easiest approach in a numerical calculation is to start at a field value sufficiently higher than the field at which the Zeeman energy fully overcomes the anisotropy energy – in the sense that there is only one minimum and one maximum left in the energy landscape – and to assume that the magnetization is parallel to the applied field in this configuration. This approach was implemented and found to be very accurate in [12](#) for fitting FMR spectra recorded at different microwave frequencies. Figure [4](#) shows some calculated spectra using the solution presented above, with the corresponding equilibrium angles calculated with this trajectory dependent algorithm. The overall calculation time was about five minutes for 540180 data points.

Equation [9](#) in combination with eq. [13](#) describe a very fast algorithm to calculate the complete susceptibility for any given free energy density and any measurement trajectory. This algorithm however will not always align the magnetization in the absolute minimum of the free energy, in fact it will fall into meta-stable states if for instance a fourfold crystalline anisotropy is considered and the applied field is swept along the field angle rather than the field amplitude, predicting the occurrence of ferromagnetic resonance in meta-stable states.

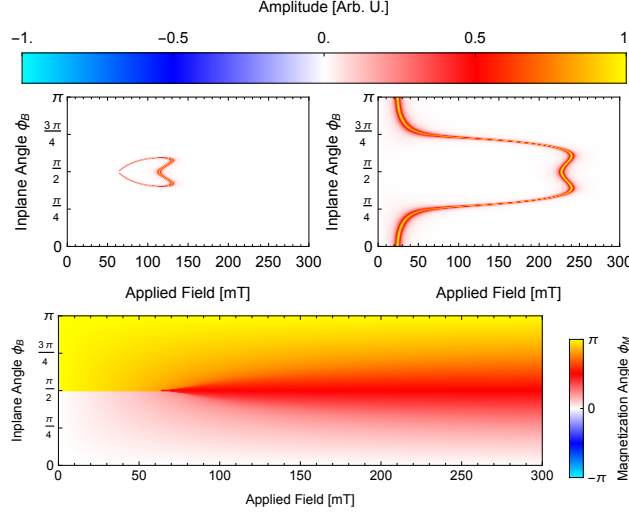


Figure 4: Calculated spectra at typical X-Band frequencies: 10 GHz (top left), and 18GHz (top right) and the corresponding solutions for the magnetization angles (bottom). The model that has been used for the free energy here is a cubic anisotropy  $K_4 = 4.8 \cdot 10^4 \text{ J/m}^3$  where the 110-direction is perpendicular to the azimuthal plane ( $\theta = \frac{\pi}{2}$ ) together with an in-plane uni-axial anisotropy  $K_u = -7.5 \cdot 10^4 \text{ J/m}^3$  and a 2-fold out of plane anisotropy  $K_2 = 0.3 \cdot 10^4 \text{ J/m}^3$  according to<sup>10</sup> with the demagnetizing tensor of a thin film. The g-factor was set to 2.09 and the damping constant of  $\alpha = 0.004$  was used.

### III. SUMMARY

We have devised a versatile analytic model, capable of accurately describing FMR experiments as well as modeling the full magnon dispersion. The model is simple in that it requires only derivatives. Condensed into a single operator  $\chi_{\text{hf}}$ , it is compact and thus easy to use in analytic and numeric applications. The formulation through an energy density allows for easy modification of the model to adapt different types of interactions, such as dipole-dipole-interaction, spin-spin-interactions like the Dzyaloshinskii-Moriya interaction and spin-orbit interactions. It can also be applied directly to spatial dependent spin configurations obtained from micromagnetic simulations to retrieve information about the magnetodynamic properties of spin textures. The model is not restricted to evaluating the magnon dispersion as a function  $\omega(k)$  but instead yields the magnonic response amplitude  $\chi(\omega, k)$  as a Green's function. In addition to this, the algorithm described in sec. II C makes it possible to apply the model on orientations of the magnetization which are non collinear with the symmetry directions of the system or the applied magnetic field. This can be used to calculate angular dependent spectra, as well as identify meta-stable states and describe their magnetodynamic

behavior.

- 
- <sup>1</sup> D. Polder, The London, Edinburgh, and Dublin Philosophical Magazine and Journal of Science **40**, 99 (1949), <http://dx.doi.org/10.1080/14786444908561215>, URL <http://dx.doi.org/10.1080/14786444908561215>.
- <sup>2</sup> L. D. Landau and J. M. Lifschitz, Phys. Zeitsch. der Sow. **8**, 153 (1935).
- <sup>3</sup> T. L. Gilbert, IEEE Transactions on Magnetics **40**, 3443 (2004), ISSN 0018-9464.
- <sup>4</sup> C. Kittel, Phys. Rev. **82**, 565 (1951), URL <http://link.aps.org/doi/10.1103/PhysRev.82.565>.
- <sup>5</sup> F. Keffer and C. Kittel, Phys. Rev. **85**, 329 (1952), URL <http://link.aps.org/doi/10.1103/PhysRev.85.329>.
- <sup>6</sup> S. V. Vonsovskii, *Ferromagnetic resonance: the phenomenon of resonant absorption of a high-frequency magnetic field in ferromagnetic substances*, International series of monographs on solid state physics (Pergamon Press, 1966), URL <https://books.google.de/books?id=oOXvAAAAMAAJ>.
- <sup>7</sup> J. O. Artman, Phys. Rev. **105**, 74 (1957), URL <http://link.aps.org/doi/10.1103/PhysRev.105.74>.
- <sup>8</sup> H. Suhl, Phys. Rev. **97**, 555 (1955), URL <http://link.aps.org/doi/10.1103/PhysRev.97.555.2>.
- <sup>9</sup> J. Smit and H. G. Beljers, Philips Research Reports **10**, 113 (1955).
- <sup>10</sup> M. Farle, Reports on Progress in Physics **61**, 755 (1998), URL <http://stacks.iop.org/0034-4885/61/i=7/a=001>.
- <sup>11</sup> V. Flovik, F. Macià, A. D. Kent, and E. Wahlström, Journal of Applied Physics **117**, 143902 (2015), URL <http://scitation.aip.org/content/aip/journal/jap/117/14/10.1063/1.4917285>.
- <sup>12</sup> R. Salikhov, L. Reichel, B. Zingsem, F. M. Römer, R.-M. Abrudan, J. Ruzs, O. Eriksson, L. Schultz, S. Fähler, M. Farle, et al., arXiv preprint arXiv:1510.02624 (2015).
- <sup>13</sup> H. Suhl, Journal of Physics and Chemistry of Solids **1**, 209 (1957), ISSN 0022-3697, URL <http://www.sciencedirect.com/science/article/pii/0022369757900100>.
- <sup>14</sup> I. E. Dzyaloshinskii, Soviet Physics JETP **5**, 1259 (1957).

- <sup>15</sup> T. Moriya, Phys. Rev. **120**, 91 (1960), URL <http://link.aps.org/doi/10.1103/PhysRev.120.91>.
- <sup>16</sup> F. Keffer, *Ferromagnetism / Ferromagnetismus* (Springer Berlin Heidelberg, Berlin, Heidelberg, 1966), chap. Spin Waves, pp. 1–273, ISBN 978-3-642-46035-7, URL [http://dx.doi.org/10.1007/978-3-642-46035-7\\_1](http://dx.doi.org/10.1007/978-3-642-46035-7_1).
- <sup>17</sup> C. Kittel, *Quantum theory of solids* (Wiley, New York, 1963).
- <sup>18</sup> J.-H. Moon, S.-M. Seo, K.-J. Lee, K.-W. Kim, J. Ryu, H.-W. Lee, R. D. McMichael, and M. D. Stiles, Phys. Rev. B **88**, 184404 (2013), URL <http://link.aps.org/doi/10.1103/PhysRevB.88.184404>.
- <sup>19</sup> A. A. Stashkevich, M. Belmeguenai, Y. Roussigné, S. M. Cherif, M. Kostylev, M. Gabor, D. Lacour, C. Tiusan, and M. Hehn, Phys. Rev. B **91**, 214409 (2015), URL <http://link.aps.org/doi/10.1103/PhysRevB.91.214409>.
- <sup>20</sup> S. M. Rezende and J. C. López Ortiz, Phys. Rev. B **91**, 104416 (2015), URL <http://link.aps.org/doi/10.1103/PhysRevB.91.104416>.